European Review for Medical and Pharmacological Sciences 2019; 23: 8630-8636

Effect of fenofibrate on diabetic retinopathy in rats *via* SIRT1/NF-κB signaling pathway

N. CHEN, K. JIANG, G.-G. YAN

Department of Ophtalmology, The Affiliated Yantai Yuhuangding Hospital of Qingdao University, Yantai, China

Ning Chen and *Kai Jiang* contributed equally to this work

Abstract. – OBJECTIVE: To explore the influence of fenofibrate on the diabetic retinopathy (DR) in rats via the sirtuin1 (SIRT1)/nuclear factor-κB (NF-κB) signaling pathway.

PATIENTS AND METHODS: A total of 30 SD rats were divided into group A (DR group), group B (fenofibrate treatment group) and group C (Healthy group). Rats in group A were intraperitoneally injected with 50 mg/kg streptozotocin (STZ) for 5 days without feeding. After fasting for 2 days, blood was drawn from the tail veins of the rats to measure blood glucose, and blood glucose ≥16.7 mmol/L represented that the model was eligible. Those in group B were injected with STZ and nourished with the mixed feed containing fenofibrate (10 mg/kg). Those in group C were intraperitoneally injected with normal saline and set as negative control group. The retinal structure of rats in the three groups was observed via immunohistochemical staining, and the apoptosis of retinal ganglion cells (RGCs) was evaluated via terminal deoxynucleotidyl transferase-mediated dUTP nick end labeling (TUNEL) assay. Moreover, the protein expressions of Sirtuin1 (SIRT1) and NF-κB were detected using immunofluorescence assay and Western blotting.

RESULTS: According to the immunohistochemical staining results, rats in group C had intact retinal nuclear layer tissues without phenomena such as fracture, disorderly arrangement, blur structures, and nerve fiber layer edema. Those in group A exhibited fracture of retinal nuclear layer tissues, disorderly arranged cells, blur retinal structures at all layers, and a quite evident nerve fiber layer edema. Compared to that in group A, the nerve fiber layer edema in group B was significantly improved. The TUNEL assay results revealed that compared to normal rats in group C, those in group A and group B had apoptotic RGCs. Additionally, the number of apoptotic cells was the largest in group A, and compared to that in group A, it was notably reduced in group B after treatment with fenofibrate. According to the immunofluorescence assay results, after being treated with fenofibrate, rats in group B showed a significantly lower protein expression level of NF-κB in the retina than in group A. Based on the Western blotting detection results, the protein expression level of NF-κB in group B was evidently lower than that in group A, and was the highest in group A and the lowest in group C. Compared to that in group C, the protein expression level of SIRT1 in group B was increased.

CONCLUSIONS: Fenofibrate facilitates the expression of SIRT1 in the retinal tissues to reduce the NF-κB activity, thereby treating DR in rats.

Key Words:
Fenofibrate, SIRT1, NF-κB, Diabetic retinopathy.

Introduction

Diabetic retinopathy (DR), an ocular complication, is not only the leading cause of vision loss in most diabetic patients, but also the primary factor for blindness in adults in developed countries and China[1,2]. Although laser therapy can help prevent and delay DR, it is less effective for severe patients. Results of epidemiological studies have indicated that the majority of diabetic patients suffer from several complications, in which DR is the most common disease, and that the key is to investigate effective approaches to effectively alleviate the disease in patients[3,4]. Sirtuin1 (SIRT1) depends on nicotinamide adenine (NAD) to deacetylate and regulate the histones, thereby affecting multiple factors in the retina. This role is evident in the induction of DR[5,6]. SIRT1, which was originally found in yeast, was a highly conservative gene with the ability of regulating energy limitation[7,8] Some studies[9,10] have found that the expression of SIRT1 is closely related to the activity of nuclear factor-κB (NF-κB), and SIRT1 influences the acetylation of NF-κB while acting on the substrate p53 to extend survival and life span. The research revealed that the onset of DR

Corresponding Author: Guigang Yan, MD; e-mail: yhdyanguigang@163.com

involves vascular endothelial growth factors, intercellular adhesion molecule-1, and E-selectin, all regulated by NF-κB[11,12]. The activity of NF-κB is enhanced in the lesion tissues and, as long as it is suppressed through interventions, diabetes mellitus will be effectively controlled. Fenofibrate is a peroxisome proliferator-activated receptor (PPAR)-α agonist that regulates blood lipid[13,14]. In recent years, medical researches have demonstrated that fenofibrate has a certain inhibitory effect on DR and plays some particular role in the progression of DR. Further studies[15,16] have shown that fenofibrate modulates the activity of superoxides to resist oxidation in retinopathy tissues, thereby repressing cell apoptosis and migration, and the activity of inflammatory factors. Therefore, in the present study, the rat model of DR was established and the comparison experiment was conducted to explore whether fenofibrate affects DR in rats *via* the SIRT1/NF-κB signaling pathway.

Materials and Methods

Modeling and Grouping

A total of 30 Sprague-Dawley (SD) rats weighing 180-200 g were purchased from Guangdong Medical Laboratory Animal Center. This investigation was approved by the Animal Ethics Committee of Qingdao University Animal Center. All the SD rats were divided into group A (DR group), group B (fenofibrate treatment group) and group C (Healthy group). Rats in group A were intraperitoneally injected with 50 mg/kg streptozotocin (STZ) for 5 days without feeding. After fasting for 2 days, blood was drawn from the tail veins of the rats to measure blood glucose, and the model with blood glucose ≥16.7 mmol/L was deemed eligible. Those in group B were injected with STZ and nourished with the mixed feed containing fenofibrate (10 mg/kg). Those in group C were intraperitoneally injected with normal saline and set as negative control group.

Main Reagents and Instruments

STZ (Enzo Biochem, USA), rat anti-NF-κB monoclonal antibody (Abcam, Cambridge, MA, USA), goat anti-rabbit IgG (Suzhou Juneng Technology, Suzhou, China), reverse transcriptions-polymerase chain reaction (RT-PCR) kit (Shanghai Superchip Technology, Shanghai, China) and NF-κB primers (Shanghai Yu Bo Biotech, Co., Ltd., Shanghai, China).

Immunohistochemical Staining of Retinas

After being fed for 2 months, rats were sacrificed *via* breaking the neck to excise the left eyeballs and completely separate the retinas. First, retinas were sealed in paraformaldehyde solution for 4 h, and with the ocular anterior segments resected, the retinas were dehydrated using ethanol according to the following steps: 75% ethanol for 1.5 h, 95% ethanol for 1.5 h, 95% ethanol for 1 h, anhydrous ethanol for 1.5 h, anhydrous ethanol for 1 h, No. 1 xylene for 0.5 h and No. 2 xylene for 0.5 h. After being paraffin-embedded, they were cut into 4 μm-thick slices and added with 3% hydrogen peroxide (H_2O_2) to inactivate endogenous enzymes. Then, the slices were sealed in 6% goat serum and incubated with the primary antibody (diluted at 1:100) at 4°C overnight. After that, products were warmed at 37°C for 45 min and incubated with the secondary antibody (diluted at 1:1000), followed by staining using diaminobenzidine (DAB) staining solution (Solarbio, Beijing, China) and counter-staining using hematoxylin. Finally, the structure of the model tissues in the three groups was observed under a high-power microscope.

Detection of Apoptosis of Retinal Ganglion Cells (RGCs) via Terminal Deoxynucleotidyl Transferase-Mediated dUTP Nick End Labeling (TUNEL)

The retinal sections were routinely embedded in paraffin, and the paraffin-embedded sections in group A, B, and C were sealed in a sealing reagent according to the instructions of TUNEL (Novus, Littleton, CO, USA) assay. Then, three pieces of retinal sections were sampled from group A, B, and C, respectively, and observed in five high-power fields of view under the fluorescence microscope to count the number of green TUNEL-positive cells and analyze apoptosis of the RGCs.

Detection of Protein Expression of NF-κB Via Immunofluorescence Assay

After digestion, the RGCs were harvested, transformed into suspension, centrifuged at 8000 rpm for 8 min and rinsed using phosphate-buffered saline (PBS) preheated at 37°C 2-3 times in the culture plate. Then, the slides on which the cells grew were washed in PBS for 3 times (3 min/time). Subsequently, they were sealed in 4% paraformaldehyde for 0.5 h, rinsed with PBS for 2-3 times and added with 0.5% Triton X-100 (prepared with PBS) to rupture the membranes

for 10 min. After that, cells were washed using PBS 2-3 times again and sealed with goat serum for 0.5 h. With the blocking solution blot up, they were incubated with the rat primary antibody at 4°C in the dark for 12 h. After the creeping slides were washed 3 times (3 min/time) using Phosphate-Buffered Saline and Tween-20 (PBST) and the excess liquid was blot up using absorbent paper, cells were added dropwise with the diluted fluorescence-labeled secondary antibody at 20-37°C in the wet box for 1 h and washed in PBST for 3 times (3 min/time). The resulting cells were added dropwise with 4',6-diamidino-2-phenylindole (DAPI; Beyotime, Shanghai, China) to stain the nuclei in the dark for 5 min, and the excess DAPI was washed away using PBST for 4 times (5 min/time). Finally, with the liquid absorbed using absorbent paper, the creeping slides were sealed in the sealing solution containing anti-fluorescence quencher and observed under the fluorescence to acquire images.

Detection of Protein Expressions of SIRT1 and NF-κB Via Western Blotting

The tissue lysate was prepared by evenly mixing an appropriate volume of radioimmunoprecipitation assay (RIPA) with phenylmethylsulfonyl fluoride (PMSF; Beyotime, Shanghai, China), a protease inhibitor, with a ratio of 100:1. Retinal tissues were isolated, sheared into pieces and lysed using the lysate. Then, tissues were placed into an Eppendorf (EP) tube, centrifuged in a low-temperature high-speed centrifugal machine at 4°C and 14,000 rpm for 30 min, and the protein supernatant was extracted. Subsequently, proteins were denatured *via* heat bath at 95°C for 10 min. The protein samples prepared were stored in the refrigerator at –80°C for later use. After quantification using bicinchoninic acid (BCA) kit (Pierce, Rockford, IL, USA), dodecyl sulfate, sodium salt-polyacrylamide gel electrophoresis (SDS-PAGE) gel was prepared, and the protein samples stored were loaded into the SDS-PAGE gel wells for electrophoresis under the constant voltage of 80 V. After electrophoresis for 2.5 h, the proteins were transferred onto polyvinylidene difluoride (PVDF) membranes (Roche, Basel, Switzerland) by the semi-dry transfer method, and the membranes were soaked in the Tris-Buffered Saline and Tween 20 (TBST) containing 5% of skim milk powder, shaken slowly using a shaking table and sealed. After sealing, they were incubated with the primary antibody diluted with 5% skim milk powder and washed using TBST for 3 times (10 min/time). Then, they were incubated with the secondary antibody at room temperature for 2 h and rinsed using TBST and TBS twice and once, respectively (10 min/time). The resulting proteins were detected using enhanced chemiluminescence (ECL) reagent and exposed in a darkroom. Their relative expression level was analyzed using the Image-Pro Plus v6 software (Media Cybernetics, Silver Spring, MD, USA).

Statistical Analysis

Statistical Product and Service Solutions (SPSS) 20.0 (SPSS, Chicago, IL, USA) software was used to statistically analyze the apoptosis of RGCs and expressions of SIRT1 and NF-κB in the three groups of rats. The *t*-test and single-factor analysis were performed for comparisons among the three groups. All the statistical results were expressed as mean ± SD, and $p<0.05$ was considered statistically significant.

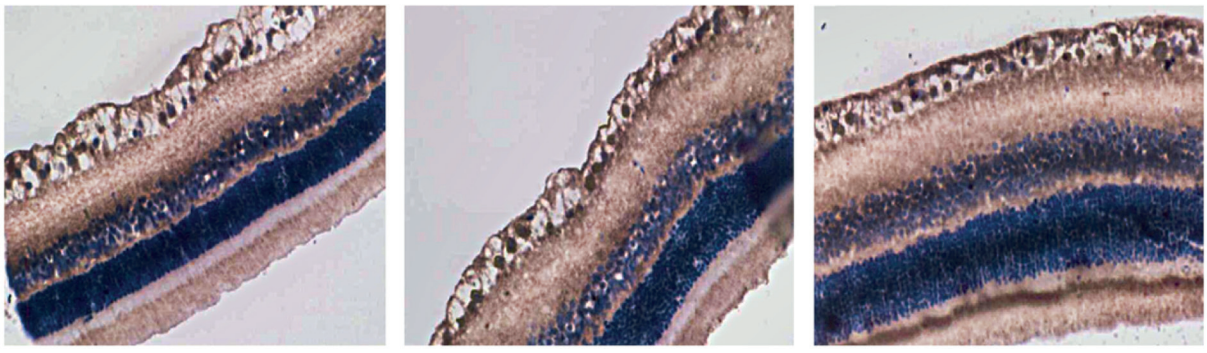

Figure 1. Changes in the structures of rat retinas in all the groups (magnification: 100×).

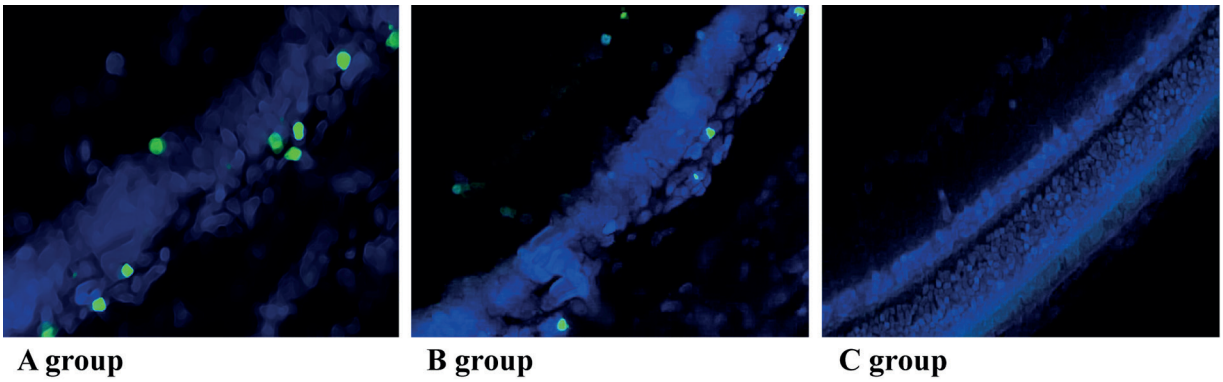

Figure 2. Changes in TUNEL-positive RGCs in each group of rats (magnification: 100×).

Results

Histomorphological Changes of Retinal Tissues Detected Via Immunohistochemical Staining

The healthy rats in group C had intact retinal nuclear layer tissues without fracture, disorderly arrangement, blur structures, and nerve fiber layer edema, while the rats in group A exhibited fracture of retinal nuclear layer tissue, disorderly arranged cells, blur retinal structures at all layers, and a quite evident nerve fiber layer edema. Compared to that in group A, the nerve fiber layer edema in group B was significantly improved. The above results indicated that fenofibrate markedly improved the histomorphology of the retinal tissues in diabetic rats (Figure 1).

Apoptosis of RGCs Detected Via TUNEL Assay

The apoptosis index of the RGCs in group A, B, and C was (13.205±1.023), (9.317±0.936) and (0.839±0.127), respectively. According to the above results, rats in group A showed more apoptotic RGCs (green fluorescence spots) than normal rats in group C and, compared to that in group A, the number of apoptotic RGCs was substantially reduced in group B after treatment with fenofibrate, showing a statistically significant difference (p<0.05) (Figures 2 and 3).

Protein Expression of NF-κB in Retinal Cells According to The Immunofluorescence Assay Results

The immunofluorescence assay results showed that the protein expression level of NF-κB in the retinal cells of rats was significantly lowered in group B after fenofibrate treatment compared to that in group A (Figures 4 and 5).

Protein Expressions of SIRT1 and NF-κB in Rat Retinas

According to the Western blotting detection results, the protein expression of NF-κB in group B was evidently lowered compared to that in group A, and it was the highest in group A and the lowest in group C (p<0.05). In addition, group A exhibited a notably lower protein expression level of SIRT1 than group B [(0.057±0.031) *vs.* (0.065±0.027)], and the protein expression level of SIRT1 in group C was higher than that in group A and group B [(0.103±0.029) *vs.* (0.057±0.031) *vs.* (0.065±0.027)] (p<0.05) (Table I and Figure 6).

Discussion

Diabetes can trigger multi-organ metabolic disorder and its complication. DR is capable of causing vision loss and keratopathy in patients, which has become the main pathogenic factor for blindness in Europe and America. The epidemiologi-

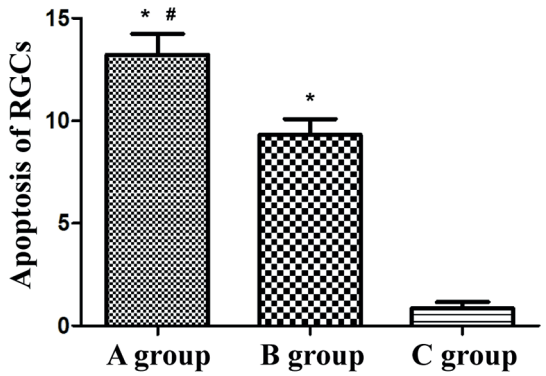

Figure 3. Apoptosis of RGCs in each group of rats. *: p<0.05, *vs.* group C and #: p<0.05, *vs.* group B.

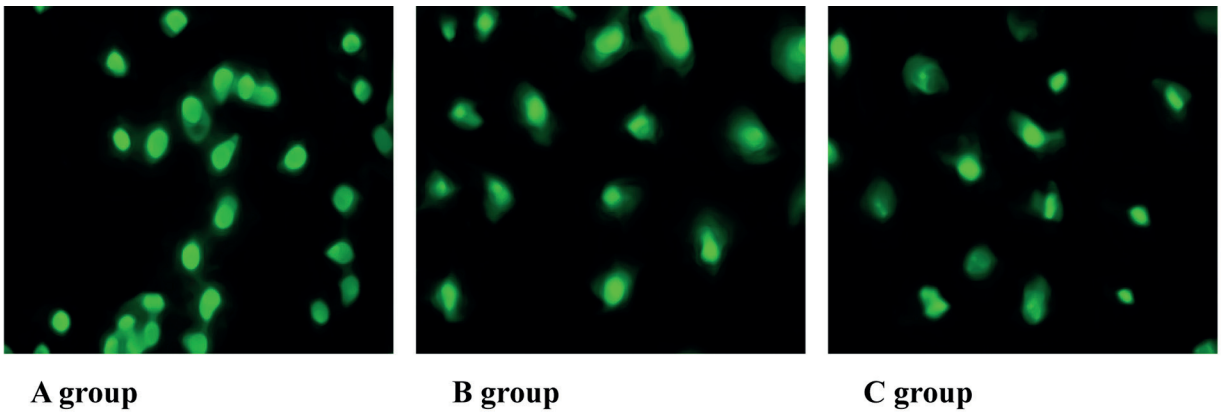

Figure 4. Protein expression of NF-κB in retinal cells detected *via* immunofluorescence assay (magnification: 40×).

Table I. Protein expressions of SIRT1 and NF-κB in retinas ($p<0.05$).

Group	SIRT1 protein	NF-κB protein
Group A (DR group)	0.057±0.031*#	0.792±0.015*#
Group B (fenofibrate treatment group)	0.065±0.027*#	0.602±0.032*#
Group C (Healthy group)	0.103±0.029*#	0.501±0.027*#

Note: *: $p<0.05$, *vs.* group C and #: $p<0.05$, *vs.* group B.

cal study results have revealed that the incidence rate of DR is gradually increasing as a growing number of elderly people suffer from diabetes[17-19]. For a long time, the occurrence of DR has been associated with hyperlipidemia and, as a PPAR-α agonist, fenofibrate modulates the expressions of liver apolipoprotein CIII mRNA, nucleus cell chemokine-1, and NF-κB *via* PPAR-α.

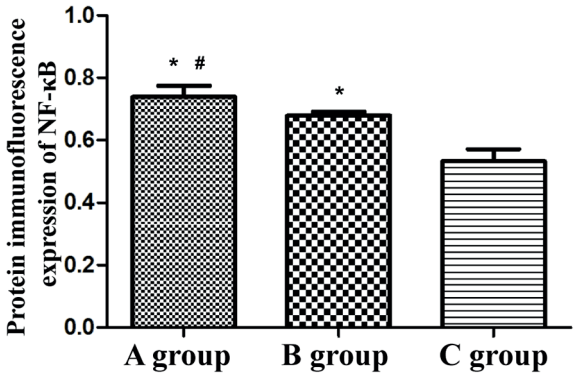

Figure 5. Protein expression of NF-κB in retinal cells detected *via* immunofluorescence assay. *: $p<0.05$, *vs.* group C and #: $p<0.05$, *vs.* group B.

According to the experimental results in the present study, the healthy rats in group C had intact retinal nuclear layer tissues without phenomena such as fracture, disorderly arrangement, blur structure, and nerve fiber layer edema, while rats in group A exhibited fracture of retinal nuclear layer tissue, disorderly arranged cells, blur retinal structures at all layers, and a quite evident nerve fiber layer edema. Compared to those in group A, the nerve fiber layer edema and the structures at all layers in group B were significantly improved, indicating that fenofibrate markedly improves the histomorphology of the retinal tissues in diabetic

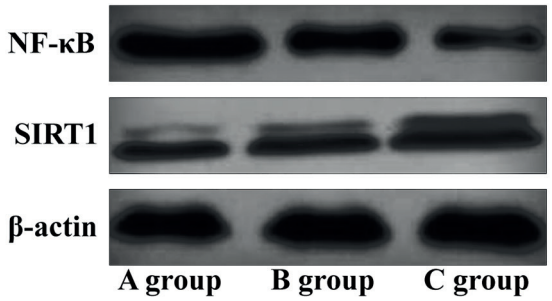

Figure 6. Protein expressions of SIRT1 and NF-κB in retinas.

rats, thereby treating DR. Pharmacological studies have found that fenofibrate activates the Nrf2 signaling pathway in the retina and inhibits the activation of NLRP3 inflammatory corpuscles to alleviate oxidative stress and neuroinflammatory response in DR, thus playing an important regulatory role in DR, which is consistent with the results in this study.

Scholars[20,21] have suggested that apoptosis of RGCs enables DR to induce vision loss in patients, and monitoring also becomes a key to the prevention of DR. According to the TUNEL assay results, the apoptosis rate of RGCs in rats in group A were the highest, and after treatment with fenofibrate, the number of apoptotic RGCs was notably reduced in group B, suggesting that fenofibrate prominently relieves cell apoptosis in the retinal tissues of diabetic rats[22,23]. The immunofluorescence assay results showed that after being treated with fenofibrate, the rats in group B had a markedly lowered protein expression level of NF-κB in the retinal cells compared to those in group A. Pordel et al[24] suggested that blocking the AGEs/RAGE/NF-κB signaling pathway can protect the retina in diabetic rats. Takizawa et al[25] have found that the activity of NF-κB is enhanced in the tissues of diabetic rats and, once suppressed through interventions, diabetes can be effectively improved. Yang et al[26] have suggested that NF-κB is abnormally activated prior to apoptosis of islet cells. The activated NF-κB affects islet cell functions to reduce the content of blood insulin, thus promoting cell apoptosis[26], which conforms to the findings of the present study. According to the Western blotting results, the protein expression of NF-κB was evidently lower in group B compared to that in group A, i.e., the highest in group A and the lowest in group C ($p<0.05$). Additionally, the protein expression level of SIRT1 in group A was substantially lower than that in group B, and it was higher in group C than in group A and group B ($p<0.05$). Studies have shown that the expression of SIRT1 is closely related to the activity of NF-κB and, once depending on NAD, it deacetylates the substrate p35 to extend survival and life span of cells[27,28]. The increase in the activity of NF-κB can induce immunosuppression, thereby triggering metabolic disorders in several organs in the whole body, including keratopathy and other comorbidities[29,30]. NF-κB is activated in ocular tissues, while SIRT1 is inactivated, resulting in keratopathy. The above result is consistent with that of the present study.

Conclusions

We showed that fenofibrate promotes the expression of SIRT1 in retinal tissues to repress NF-κB activity, thereby playing a therapeutic role in DR in rats.

Conflict of interest

The authors declare no conflicts of interest.

References

1) Liu GZ, Hou TT, Yuan Y, Hang PZ, Zhao JJ, Sun L, Zhao GQ, Zhao J, Dong JM, Wang XB, Shi H, Liu YW, Zhou JH, Dong ZX, Liu Y, Zhan CC, Li Y, Li WM. Fenofibrate inhibits atrial metabolic remodelling in atrial fibrillation through PPAR-alpha/sirtuin 1/PGC-1alpha pathway. Br J Pharmacol 2016; 173: 1095-1109.
2) Liu HW, Meng Y, Ren YB, Sun P. MicroRNA-15b participates in diabetic retinopathy in rats through regulating IRS-1 via Wnt/β-catenin pathway. Eur Rev Med Pharmacol Sci 2018; 22: 5063-5070.
3) Kim MY, Lim JH, Youn HH, Hong YA, Yang KS, Park HS, Chung S, Ko SH, Shin SJ, Choi BS, Kim HW, Kim YS, Lee JH, Chang YS, Park CW. Resveratrol prevents renal lipotoxicity and inhibits mesangial cell glucotoxicity in a manner dependent on the AMPK-SIRT1-PGC1α axis in db/db mice. Diabetologia 2013; 56: 204-217.
4) Noureldein MH, Abd El-Razek RS, El-Hefnawy MH, El-Mesallamy HO. Fenofibrate reduces inflammation in obese patients with or without type 2 diabetes mellitus via sirtuin 1/fetuin A axis. Diabetes Res Clin Pract 2015; 109: 513-520.
5) Gao S, Liu W, Zhuo X, Wang L, Wang G, Sun T, Zhao Z, Liu J, Tian Y, Zhou J, Yuan Z, Wu Y. The activation of mTOR is required for monocyte pro-inflammatory response in patients with coronary artery disease. Clin Sci (Lond) 2015; 128: 517-526.
6) Remels AH, Gosker HR, Schrauwen P, Langen RC, Schols AM. Peroxisome proliferator-activated receptors: a therapeutic target in COPD? Eur Respir J 2008; 31: 502-508.
7) Brandstädt S, Schmeisser K, Zarse K, Ristow M. Lipid-lowering fibrates extend C. elegans lifespan in a NHR-49/PPARalpha-dependent manner. Aging (Albany NY) 2013; 5: 270-275
8) Phuntuwate W, Suthisisang C, Koanantakul B, Chaloeiphap P, Mackness B, Mackness M. Effect of fenofibrate therapy on paraoxonase1 status in patients with low HDL-C levels. Atherosclerosis 2008; 196: 122-128.
9) Haak T, Haak E, Kusterer K, Weber A, Kohleisen M, Usadel KH. Fenofibrate improves microcirculation in patients with hyperlipidemia. Eur J Med Res 1998; 3: 50-54.
10) Gureev AP, Shmatkova ML, Bashmakov VY, Starkov AA, Popov VN. [The effect of fenofibrate on ex-

pression of genes involved in fatty acids beta-oxidation and associated free-radical processes]. Biomed Khim 2016; 62: 426-430.

11) Wang Y, Wang DS, Cheng YS, Jia BL, Yu G, Yin XQ, Wang Y. Expression of microRNA-448 and SIRT1 and prognosis of obese type 2 diabetic mellitus patients after laparoscopic bariatric surgery. Cell Physiol Biochem 2018; 45: 935-950.

12) Zhou CH, Zhang MX, Zhou SS, Li H, Gao J, Du L, Yin XX. SIRT1 attenuates neuropathic pain by epigenetic regulation of mGluR1/5 expressions in type 2 diabetic rats. Pain 2017; 158: 130-139.

13) Tang K, Sun M, Shen J, Zhou B. Transcriptional coactivator p300 and silent information regulator 1 (SIRT1) gene polymorphism associated with diabetic kidney disease in a chinese cohort. Exp Clin Endocrinol Diabetes 2017; 125: 530-537.

14) Kowluru RA, Mishra M, Kumar B. Diabetic retinopathy and transcriptional regulation of a small molecular weight G-Protein, Rac1. Exp Eye Res 2016; 147: 72-77.

15) Zhao S, Li T, Li J, Lu Q, Han C, Wang N, Qiu Q, Cao H, Xu X, Chen H, Zheng Z. MiR-23b-3p induces the cellular metabolic memory of high glucose in diabetic retinopathy through a SIRT1-dependent signalling pathway. Diabetologia 2016; 59: 644-654.

16) Gupta A, Uribarri J. Dietary advanced glycation end products and their potential role in cardiometabolic disease in children. Horm Res Paediatr 2016; 85: 291-300.

17) Kowluru RA, Santos JM, Zhong Q. Sirt1, a negative regulator of matrix metalloproteinase-9 in diabetic retinopathy. Invest Ophthalmol Vis Sci 2014; 55: 5653-5660.

18) Hou BY, Li L, Zhang L, Du GH. [The role of SIRT1 in the treatment of diabetic nephropathy]. Yao Xue Xue Bao 2014; 49: 1625-1630.

19) Wang Y, Zhao X, Shi D, Chen P, Yu Y, Yang L, Xie L. Overexpression of SIRT1 promotes high glucose-attenuated corneal epithelial wound healing via p53 regulation of the IGFBP3/IGF-1R/AKT pathway. Invest Ophthalmol Vis Sci 2013; 54: 3806-3814.

20) Yu W, Wan Z, Qiu XF, Chen Y, Dai YT. Resveratrol, an activator of SIRT1, restores erectile function in streptozotocin-induced diabetic rats. Asian J Androl 2013; 15: 646-651.

21) Fagan XJ, Chong EW. Fenofibrate and diabetic retinopathy. Clin Exp Ophthalmol 2015; 43: 297-299.

22) Dingwell KS, Holt CE, Harris WA. The multiple decisions made by growth cones of RGCs as they navigate from the retina to the tectum in Xenopus embryos. J Neurobiol 2000; 44: 246-259.

23) Valiente-Soriano FJ, Nadal-Nicolás FM, Salinas-Navarro M, Jiménez-López M, Bernal-Garro JM, Villegas-Pérez MP, Agudo-Barriuso M, Vidal-Sanz M. BDNF rescues RGCs but not intrinsically photosensitive RGCs in ocular hypertensive albino rat retinas. Invest Ophth Vis Sci 2015; 56: 1924.

24) Pordel S, Nemati K, Karimi MH, Doroudchi M. NF-κB1 Rs28362491 mutant allele frequencies along the silk road and beyond. Iran J Public Health 2018; 47: 397-406.

25) Takizawa Y, Kosuge Y, Awaji H, Tamura E, Takai A, Yanai T, Yamamoto R, Kokame K, Miyata T, Nakata R, Inoue H. Up-regulation of endothelial nitric oxide synthase (eNOS), silent mating type information regulation 2 homologue 1 (SIRT1) and autophagy-related genes by repeated treatments with resveratrol in human umbilical vein endothelial cells. Br J Nutr 2013; 110: 2150-2155.

26) Yang CM, Chen YW, Chi PL, Lin CC, Hsiao LD. Resveratrol inhibits BK-induced COX-2 transcription by suppressing acetylation of AP-1 and NF-κB in human rheumatoid arthritis synovial fibroblasts. Biochem Pharmacol 2017; 132: 77-91.

27) Deng Z, Jin J, Wang Z, Wang Y, Gao Q, Zhao J. The metal nanoparticle-induced inflammatory response is regulated by SIRT1 through NF-κB deacetylation in aseptic loosening. Int J Nanomedicine 2017; 12: 3617-3636.

28) Zheng H, Fu Y, Huang Y, Zheng X, Yu W, Wang W. mTOR signaling promotes foam cell formation and inhibits foam cell egress through suppressing the SIRT1 signaling pathway. Mol Med Rep 2017; 16: 3315-3323.

29) Cai Y, Li W, Tu H, Chen N, Zhong Z, Yan P, Dong J. Curcumolide reduces diabetic retinal vascular leukostasis and leakage partly via inhibition of the p38MAPK/NF-κB signaling. Bioorg Med Chem Lett 2017; 27: 1835-1839.

30) Khan Z, Kuriakose RK, Khan M, Chin EK, Almeida DR. Efficacy of the intravitreal sustained-release dexamethasone implant for diabetic macular edema refractory to anti-vascular endothelial growth factor therapy: meta-analysis and clinical implications. Ophthalmic Surg Lasers Imaging Retina 2017; 48: 160-166.